Biogeosciences Discuss., 10, 4887–4925, 2013
www.biogeosciences-discuss.net/10/4887/2013/
doi:10.5194/bgd-10-4887-2013

Biogeosciences Discussions
Open Access

A bio-optical model for remote sensing of Lena water

H. Örek[1], R. Doerffer[1], R. Röttgers[1], M. Boersma[2], and K. H. Wiltshire[2]

[1]Helmholtz-Zentrum Geesthacht, Centre for Materials and Coastal Research, Institute of Coastal Research, Max-Planck-Str. 1., 21502 Geesthacht, Germany
[2]Alfred Wegener Institute for Polar and Marine Research, Biologische Anstalt Helgoland, P.O. Box 180, 27483 Helgoland, Germany

Received: 18 January 2013 – Accepted: 11 February 2013 – Published: 11 March 2013

Correspondence to: H. Örek (hasan.oerek@hzg.de)

Published by Copernicus Publications on behalf of the European Geosciences Union.

Abstract

Bio-optical measurements and sampling were carried out in the delta of the Lena River (Northern Siberia, Russia) during the high water run-off period between 26 June 2011 and 4 July 2011. The aim of this study was to determine the inherent optical properties of the Lena water, i.e. absorption, attenuation and scattering coefficients, during the period of maximum run-off. In this context CDOM (Colored Dissolved Organic Matter), total particle absorption, total suspended matter and phytoplankton-pigments were measured. CDOM was found to be the most dominant parameter affecting the optical properties of the river, with an absorption coefficient of 4.5–5 m^{-1} at 442 nm, which was almost four times higher than total particle absorption values at visible wavelength range during the first week of the campaign. This difference decreased over the following days when Total Suspended Matter (TSM) concentration increased. The wavelength dependent absorption spectra of the water constituents were characterized by determining the semi logarithmic spectral slope. Mean CDOM, and Detritus slopes, were 0.0149 nm^{-1} (stdev = 0.0003, $n = 18$), and 0.0057 nm^{-1} (stdev = 0.0017, $n = 19$), respectively, values which are typical for water bodies with high concentrations of dissolved and particulate carbon. Mean total chlorophyll *a*, and total suspended matter, were also measured to determine the relationship between concentrations and optical properties. Mean chlorophyll *a* and total suspended matter were 1.821 mg m^{-3} (stdev = 0.734 $n = 18$) and 31.89 mg L^{-1} (stdev = 19.94) respectively. The light penetration depth (Secchi disc depth) was highly correlated with the suspended matter concentration with a maximum of 90 cm. We conclude that the bio-optical properties of the Lena River are rather complex because of the high CDOM and variable particle load which may change within a matter of days. Furthermore, the chlorophyll concentration constitutes a small fraction. Our results will improve the remote sensing protocols of the river and coastal waters in and around the Lena Delta and serve as a basis for characterizing the light climate with respect to primary production.

BGD
10, 4887–4925, 2013

1 Introduction

The Lena River with its extensive delta is the pathway of transporting large amounts of organic and inorganic material in a a diverse array molecular forms of carbon from its huge catchment area into the Arctic Ocean, particularly into the Laptev Sea (Kattner et al., 1999). This input may increase with the thawing Siberian permafrost due to global warming. Permafrost thawing and diminishing sea ice coverage are distinctive indicators of global warming in the Arctic (Walsh, 1991; Payette et al., 2004; Morison at al., 2012). Concomitantly changes in hydrographic and meteorological conditions have been observed in the Lena Delta, which in turn influence the Arctic Ocean (Morison at al., 2012). Considerable water budget, geomorphologic and ecosystem changes are expected in the near future (McClelland et al., 2006; Dmitrenko et al., 2008; Morison at al., 2012). However, it is not so easy to predict future of the Lena Delta, with the current lack of present, past and perhaps most importantly continuous data. Gathering of relevant data is not always possible by in-situ sampling, in such inaccessable areas like the Lena Delta. Thus remote sensing tools are crucial to the understanding of the current state and for continuous monitoring. Remote sensing can also not be used as "stand alone" tool until it is verified and corrected with in-situ measurements.

The eastern part of the Arctic region is less well studied than the Western part. Remoteness, harsh conditions and lack of scientific infrastructure are the main causes for this lack of knowledge, especially for the Lena region. However, knowledge about the role of the Lena is essential in order to understand the Laptev Sea and the Arctic Ocean in general. Therefore, for the understanding of biogeochemical cycles, the to quantification and analyses of the temporal and spatial patterns of the input of carbon and sediment by Siberian Rivers to the Arctic Basin. The Lena has an enormous catchment area of about 2 486 000 km^2, which is mainly characterised by Siberian forests, tundra and permafrost regions. It has an annual discharge of fresh water of around 500 km^3 (Dmitrenko et al., 2008, http://www.feow.org/ecoregion_details.php?eco=608.

BGD
10, 4887–4925, 2013

Previous studies in the Lena Delta region related to optical properties, mainly focused on the characterization and quantification of CDOM; POM, phytoplankton distribution and primary production (Cauwet and Sidorov, 1996; Heiskanen and Keck, 1996; Sorokin and Sorokin, 1996; Kattner et al., 1999, Gueguen et al., 2005). Studies which were done in the Laptev Sea were mostly limited to the oceanic parts, and do not include the Lena River itself or its region of coastal freshwater influence. Thus, the Lena River ecosystem is not well documented in terms of bio-optical properties. According to limited previous studies, the carbon budget of the Lena River varies a great deal. During the flood period TOC (Total organic carbon) can be up to 14.4 $g\,m^{-3}$ (June–July), while during the low water level period (November–April) this value is reported to be around 3.97 $g\,m^{-3}$, and the annual mean concentration is 10.2 $g\,m^{-3}$ (Cauwet and Sidorov, 1996). Along the river the TOC concentration remains almost constant from Yakutsk (2000 km) to the Laptev Sea (Lara et al., 1998). Turbidity of the water is higher during the flood period with concentrations of suspended matter dry weight of 50–70 $mg\,L^{-1}$. The concentration of phosphate was found to be similar to other Arctic rivers but silicate and nitrate are three times higher (Cauwet and Sidorov, 1996).

The Phytoplankton community of the Lena River is dominated by fresh water diatoms and picocyanobacteria (Heiskanen and Keck., 1996; Sorokin and Sorokin., 1996). Reported wet weights of the dominant groups and size fractioned chlorophyll concentrations are given below (Table 1).

Bio-optical data of the Lena River are scarce. In some studies Secchi disk depth and light attenuation coefficients were measured or calculated (Sorokin and Sorokin., 1996). However, the DOM (dissolved organic matter) composition in the Lena is well documented, which gives an idea of the wavelength slopes of CDOM and particles (Lara et al., 1998; Kattner et al., 1999; Lobbes et al., 2000). Particulate matter of the Lena River is composed of a lithogenic fraction, which stems from erosion by the river, and of detritus, which is formed mainly by the debris of organisms. Phytoplankton contributes only with a few percent to the total particulate matter. Main sources of Total

BGD
10, 4887–4925, 2013

suspended matter (TSM) are eroded land and the thawing permafrost (Rachold et al., 1996; Lobbes et al., 2000).

Similar studies, but in the Kara Sea, about optical properties, remote sensing and carbon content were carried by Pozdnyakov et al. (2005), Hessen et al. (2010) and Korosov et al. (2011).

The goal of our study was to determine the optical properties of the Lena river water during the period of maximum river run-off, i.e. when most of the annual water load is transported into the Laptev Sea. Using the observations the intention was to set up a bio-optical model, which describes the dominant components, which determine the optical properties, the ranges of their concentrations, their absorption and scattering spectra and the relationships between concentrations and the optical coefficients. A bio-optical model is the basis for optical remote sensing and phytoplankton studies. The selected investigation site was the entrance of the Lena Delta, where the river water is divided and flows via many arms into the coastal sea. The period and site of our investigation was selected to match the maximum concentrations of water constituents before they are spread into the coastal sea. Unfortunately the maximum water level was earlier in 2011 than usual, so that we just missed the extreme phase by 7–10 days, which gave us the possibility to study both the end of the high-water period as well as the beginning of the summer period, thus yielding information on more different situations.

2 Investigation site and methods

All measurements were carried out in the vicinity of the Samoylov Island, which is located at the entrance of the delta (Fig. 1). Daily water samples were collected from the Lena River stream two times a day. First sampling point was located at the Samoylov Island coast (Fig. 1., station 2, Table 2), The second sampling location (Fig. 1., station 1, Table 1) was in the main stream of the Lena, close to the small rock island of Stolp. Samples were taken from a small boat. In addition to these positions another branch

BGD
10, 4887–4925, 2013

of the Lena River, was sampled once (Fig. 1, stations 3–6, Table 1). Samples were taken usually between 10:30 and 15:30 local time when the sun elevation is relatively high and overpasses of the ENVISAT satellite were expected. At the time of sampling, we measured water and air temperatures, Secchi disk depths, reflectance spectra, phytoplankton fluorescence profiles and GPS-coordinates (Table 1).

All samples were processed at Samoylov research station. Filters were prepared for measuring particle absorption, total suspended matter dry weight and phytoplankton pigment concentrations by HPLC later in the laboratory. 200 to 1500 mL of the water samples were filtered through pre-combusted GF/F filters and were kept in a deep freezer (−18 °C) until transfer in the freezer to Germany. These samples were analyzed as soon as received from Siberia 6–7 months later, to prevent or reduce further degradation of the biological material.

The absorption and scattering spectra of the fresh samples were measured before and after filtration at Samoylov using a Wetlabs hyperspectral absorption-attenuation (ACS) meter. Using these measurements the absorption and scattering coefficients of particulate matter and the dissolved fraction (CDOM) could be determined.

3 Measurements and post processing

The ACS is designed for in situ measurements. It has two different cuvettes, one for measuring the beam attenuation coefficient c and the other for measuring the absorption coefficient a. For measuring the samples at the station the instrument was installed in the lab and fixed to the bench leg (90°) Silicon tubes were attached to the inlets of the cuvettes and the samples were poured from the lower inlet to avoid or minimize bubbles (schematic setup can be found in Sullivan et al., 2006). The absorption and beam attenuation spectra were recorded. Three replicates were measured for each sample together with a blank, which was recorded between the individual measurements to check the stability of the instrument. Temperature and scattering corrections were done by post processing of the raw data (Zaneveld et al., 1994; Sullivan et al.,

BGD
10, 4887–4925, 2013

2006; Boss et al., 2009). Blank values were not used for the calculations, because it was not possible to produce or store optically clean water at the station; instead previous blank values – measured before the campaign – were used for post processing of the raw data. However, this step was not critical, since blanks are less important for such highly absorbing water bodies, where uncertainties induced by scattering of suspended matter can be up to 80 % (Boss et al., 2004).

The spectral shape of total absorption and that of the filtered water, which represents the dissolved fraction of organic matter (CDOM), were parameterized by an exponential curve, a method which was introduced already by Jerlov in 1957. The spectral slope of the semi-logarithmic CDOM curve, calculated according to Eq. (1) with a reference wavelength λ_0, is variable and depends on the kind of matter. Thus, it is an important parameter for the characterization of CDOM.

$$a(\lambda) = a(\lambda_0)\exp\{-s(\lambda - \lambda_0)\} \quad (1)$$

where a = absorption, λ = Wavelength, λ_0 = reference wavelength and s = spectral slope.

At each station Secchi disc depth was determined. Due to the low transparency of Lena water and the high current speed a standard device with a marked cable could not be used. Instead a white disc was mounted at the tip of a pole of 2 m length, which was marked with a centimeter scale. This pole was deployed from the boat by hand.

The absorption of particulate matter was measured using the filter pad technique, which is has become a standard method to determine the absorption spectra of total suspended matter, detritus and phytoplankton (details can be found: Mitchell et al., 2000). The main difficulty of the filter pad technique is the aggregating of particles in a small cross-section, reasoning an artificial amplification of absorption. This amplification is corrected by an amplification factor. In this study we used the method of measurement and correction described in Röttgers and Gehnke (2012). Measurements were done in a dual-beam UV/VIS spectrophotometer (Lambda 800, Perkin Elmer) that was equipped with a 150 mm integrating sphere (Labsphere Inc.). A piece of filter

BGD
10, 4887–4925, 2013

($\sim 1 \times 2\,cm^2$) was cut out and placed in the centre of the integrating sphere. The filter was thawed for 30–45 min before the measurement. Measured filter pieces were then bleached (hypochlorite bleach solution) for several minutes to destroy the phytoplankton pigments. Blanks were treated with the same procedure. The bleached filters gives the absorption by detritus also called non algal particulate matter directly, while the difference between untreated and bleached filters provides the absorption spectra of phytoplankton pigments. The absorption spectra are resembled to the CDOM curves and analyzed in the same way. The wavelength exponent of the absorption spectra of detritus was computed with the same equation (Eq. 1) as used for CDOM. The reference wavelength was 442 nm in both cases. Dissolved organic carbon (DOC) was measured after filtering the water through a GF/F filter. The samples were then acidified by the addition of 100 µL of HCl (25 %) before being sealed and stored in a dark fridge at 4 °C until analysis (Elementar Analysensysteme vario TOC cube; www.elementar.de). All of the glassware used in the preparation of the DOC samples was previously washed in 10 % HCl and rinsed with ultrapure water (Milli-Q Integral Water Purification System, Millipore). Particulate Organic Carbon was measured using the frozen filters. The carbon content of the samples was measured with an Elementar vario MICRO cube CHN analyser.

Absorption and scattering are the main IOPs (Inherent Optical Properties) and other variables can be derived from them. The wavelength dependent total scattering coefficients are obtained by subtracting total absorption (CDOM + water + particle) from the beam attenuation c with $c = a + b$ where c is the beam attenuation coefficient, a is the absorption and b is the scattering coefficient. By using b, single scatter albedo $\omega_0'(\omega_0 = b/c)$ can be calculated. Single scatter albedo is an useful parameter to describe the optical properties.

Phytoplankton pigments were determined using HPLC (High performance liquid chromatography) by the method developed by Zapata et al. (2000). 29 different pigments, including chlorophylls and degradation products could be separated out from the Lena samples. Pigment concentrations were computed from the area of the concentration

BGD
10, 4887–4925, 2013

peaks relative to pigment standards (DHI and Sigma). Filters were extracted for 24 h at −40 °C with 100 % Acetone (Chromatography grade), then filtered through Whatman Spartan 13 mm Ø, 0.2 µm pore size filters and transferred to the vials for chromatography.

Total suspended matter (TSM) dry weight was determined by filtering the sample water through pre-combusted (450 °C) and pre-weighted GF/F filters. The pore size of these filters defined the separation of dissolved and particulate matter for this study. The filters were weighed, after drying at 60 °C for 24 h and cooled to room temperature in a desiccator to prevent any change in weight due to humidity. The difference between the pre- and post filter weights divided by filtered sample volume resulted in the dry weight of suspended matter per unit water volume.

4 Results

4.1 Absorption

CDOM is the main source of absorption in the visible wave length range in the Lena River. During the first week of our campaign CDOM absorption was almost uniform within the sampling area (Fig. 2a). We observed very low variability in the CDOM absorption in the wavelength range (400–500 nm) (as indicated by the very low standard deviations in Fig. 2a), the decrease in absorption at 442 nm over time (Fig. 3) is not significant. Variability of absorption at 442 nm was in the range 4.25–5.25 m^{-1}, with standard deviation of ±0.36 m^{-1}. Contrary to this slight decrease, an increasing trend of the spectral slope was found (Fig. 4, Table 3). Spectral slopes varied between 0.0142 and 0.0158 with a standard deviation of ±0.0003. No extreme variations were observed within the sampling period..

The absorption coefficients of Total Suspended Matter (TSM) and of its detrital fraction (after bleaching) are very close to each other (Fig. 2b and c, respectively). Thus, the difference between both, which is the absorption by phytoplankton pigments, is low and noisy and therefore not represented here.

BGD
10, 4887–4925, 2013

The absorption by TSM increased by a factor of 3 during the sampling period (Fig. 3, Table 3). The spectral slopes of detritus absorption are listed in Table 3. A decreasing trend of these slopes were observed over the sampling period, except for stations 3–6, which were located in a tributary deviate of the main Lena stream, Kurungnakh arm, while all other samples were collected from the main stream and off Samoylov Island (Fig. 1). Slopes of the four Kurungnakh stations are almost double as high as those of the other samples (Fig. 5). Main stream slopes varied from 0.0038 to 0.0062, whereas, Kurungnakh station slopes varied in between 0.0089 and 0.0083.

4.2 Phytoplankton pigments

The major pigments, which we found in phytoplankton of the Lena River during our campaign, were chlorophyll *a*, Fucoxanthin (Fuco) and chlorophyll *b* (chl *b*). Diadinoxanthin (Diadino), Alloxanthin (Alloxan), Zeaxanthin (Zeaxan), and Lutein are found in lower concentrations at all stations. Some other pigments like chlorophyll *c*1, *c*2 (chl *c*1, *c*2), Neoxanthin (Neoxan)and Violoxanthin (Viola) were not always found and it present then at lower concentrations (Fig. 6). Total chlorophyll was calculated by summing up chlorophyll *a* and its all degradation products. Degradation products added 33 % (min. 15 %, max. 50 %) to total chlorophyll in average. Relatively high concentrations of Fucoxanthin and chlorophyll *b* indicate that the majority of the species in the Lena River were composed of green algae (Chlorophyta) and diatoms (Bacillariophyta).

4.3 Total suspended matter

Total suspended matter concentration was spatially and temporally variable during the sampling period. Samples, which were taken from the Kurungnakh arm (stations 3–6, Fig. 1), were lower than the samples of the main channel (Fig. 7). During the observation period concentrations of TSM increased by a factor of four and reached its maximum during our observation period at the last days of the campaign.

BGD
10, 4887–4925, 2013

4.4 Carbon concentrations

The concentration of dissolved organic carbon (DOC) was constant over the observation period in June/July at all stations with values around $9.4 \pm 0.45\,g\,m^{-3}$ when omitting one value at $16\,g\,m^{-3}$. But these values were double that of measurements in the second half of August 2011 at the same stations with values around $4.6 \pm 0.46\,g\,m^{-3}$ with $n = 38$, also when omitting one potential erroneous value at $16\,g\,m^{-3}$ (data not included in the publication).

In contrast the values of the sum of organic and inorganic particulate carbon were much more variable. During the campaign in June/July particle carbon (PC) values were in the range 0.3–$1.9\,g\,m^{-3}$ with a mean of $0.85 \pm 0.44\,g\,m^{-3}$, $n = 26$. In the second half of August these values were more variable with a range of 0.2–$6.0\,g\,m^{-3}$ and a mean of $1.07 \pm 1.08\,g\,m^{-3}$, $n = 36$.

4.5 Beam attenuation and scattering

The variability of the beam attenuation coefficient c of the Lena River water was determined mainly by the total particle absorption, since the CDOM absorption was relatively constant (Fig. 8a and b). Similar to TSM dry weight the beam attenuation coefficient increased by a factor of four during the observation period. (Fig. 8a and b).

The scattering coefficient b was determined by subtracting the total absorption (dissolved and particle fraction) from the beam attenuation coefficient (Fig. 9a). The temporal variability of the scattering coefficients was almost the same as the beam attenuation, while the absorption coefficients were less variable.

5 Discussion

A main question concerning our investigations about the bio-optical properties of the Lena water is how the results compare to other Arctic rivers and estuaries and, as a consequence, if a generic bio-optical model can be derived for optical remote sensing

BGD
10, 4887–4925, 2013

of the coastal waters of the Arctic Sea in total. Beside the Lena the major rivers, which determine the fresh water flux into the Arctic Sea, are Yenisei, Ob and Mackenzie.

Most striking is the high concentration of humic substances, which dominates the optical properties of all of these estuaries. The dissolved organic carbon (DOC) concentrations of Ob and Yenisei, close to the mouth, where the river water is not diluted by marine water, is in the range of 5–10 g C m^{-3} with extreme values of 15 g C m^{-3}, while the concentrations in the Kara Sea, where salinity exceeds 30 ppt, is < 1 g C m^{-3} (Korosov et al., 2011, also reported by Hessen et al., 2010). The concentrations, we found during our campaign in the fresh water region of the Lena were in the range 8.5–10.5 g C m^{-3} and thus corresponds to those of Ob and Yenisei.

DOC was constant over the observation period in June/July at all stations with values around 9.4 ± 0.45 g m^{-3} when omitting one value at 16 g m^{-3}. But these values were double that of measurements in the second half of August 2011 at the same stations with values around 4.6 ± 0.46 g m^{-3} with $n = 38$, also when omitting 1 value at 16 g m^{-3} (data not included in the publication).

In contrast the values of the sum of organic and inorganic particulate carbon were much more variable. During the campaign in June/July PC values were in the range 0.3–1.9 g m^{-3} with a mean of 0.85 ± 0.44 g m^{-3}, $n = 26$. In the second half of August these values were more variable with a range of 0.2–6.0 g m^{-3} and a mean of 1.07 ± 1.08 g m^{-3}, $n = 36$.

The absorption coefficients of CDOM are easier to compare. In the paper of Hessen et al. (2010) the downwelling irradiance attenuation coefficient k_d is included for some wavelengths in the UV spectral range, which are around 10 m^{-1} for 380 nm for Ob and Yenisei. Since for highly absorbing water k_d is mainly determined by the absorption coefficient, it can be transferred to an absorption coefficient of 4 m^{-1} at 442 nm assuming a spectral slope of 0.015. For the Lena we found the corresponding coefficient in the range 4–5 m^{-1}.

Absorption coefficients for the Mackenzie delta (Canada) are reported in Bélanger et al. (2006). Values close to the coast but already offshore, is in the range of 4.5–5.4 m^{-1}

BGD
10, 4887–4925, 2013

at 330 nm with a spectral slope around 0.02. The corresponding values for 442 nm using this slope would be 0.45–0.55 m^{-1}.

Mean spectral slopes of the absorption coefficients are available for the Great Whale River and Mackenzie River in the Canadian Arctic (Retamal et al., 2007). They are 0.016 m^{-1} and 0.0185 m^{-1} respectively. However, they were derived from the wavelength range 300–650 nm with a reference wavelength of 320 nm. Also the spectral slopes in Bélanger et al. (2006) with values in the range of 0.019–0.02 have obviously derived from the UV part of the spectrum (but not explicitly mentioned in the paper). Similar CDOM spectral slopes values can be found in different coastal and river waters worldwide. Helms et al. (2008), from Great Dismal Swamp and Suwannee River have reported values between 0.0158–0.0186 m^{-1}. Mean CDOM spectral slope of Elbe river water are reported to be 0.0188 (HZG Unpublished data) or 0.014 (Doerffer, 1979). More reports of this parameter can be found in Wozniak and Dera (2007). Slopes of CDOM, which we found for the Lena, are in the range 0.0145–0.0155. They were derived from the spectral rang 400–500 nm, which is the most relevant part for optical remote sensing.

Variability of the bleached TSM slopes (range 0.004–0.009) can be attributed to the particle size and/or composition and content of organic carbon (detritus), while the main stream concentrations are not co-varying with the spectral slopes. The spectral slopes are lower compared to mean Baltic and North Sea detritus absorption slopes, which are 0.013 and 0.0116 respectively (Babin et al., 2003). Ferrari et al. (2003) reported for the Baltic See values between 0.0095 and 0.0125.

Phytoplankton pigments found are similar to previous studies done in the Lena River (Heiskanen and Keck., 1996, Sorokin and Sorokin., 1996). Total chlorophyll *a* concentration was variable within our sampling period with values between 0.5 and 3 mg m^{-3}. The time series does not show any trend during our campaign. Also, the samples of the Kurungnakh river arm are not different from the major river. These values fit very well to the values of Hessen et al, 2010 for Ob (0.4–3.4 mg m^{-3}) and Yenisei (0.6–2.9 mg m^{-3}). Chlorophyll values derived from satellite data are in most cases overestimated due to

BGD
10, 4887–4925, 2013

the difficult separation between DOC and phytoplankton pigment absorption spectra (Heim et al., 2013). In Hessen et al. (2010) chlorophyll values derived from MODIS data are up to 15 mg m^{-3} for the Yenisei and up to 8 mg m^{-3} for the Ob. The chlorophyll values derived from MERIS data (Korosov et al., 2011) are even higher with values up to 30 mg m^{-3} for Ob and Yenisei.

The concentration of total suspended matter (TSM) was variable in the Lena River and side arms, mainly due to in water turbulence. It ranged from 10–60 g m^{-3} during the observation period and was not co-varying with the chlorophyll concentration (Fig. 7). Due to the high variability, which depends on local currents, water depths, river run-off, a direct comparison with corresponding snapshot observations of other Arctic rivers does not help to assess these values.

The calculated single scattering albedo of the Lena River was lower in the short and higher in the long wavelength range. This effect is caused by the strong absorption by CDOM at shorter wavelength (Fig. 9b), which reduces the number of photons to be scattered at these wavelengths. The spectrum of scattering coefficient shows an increase in the short wavelength range and remains flat at longer wavelengths (Fig. 9a). This type of spectral shape is determined by the particle composition and concentration. Especially small lithogenic particles can increase the scattering coefficients (Whitmire et al., 2007).

The relationship between the TSM dry weight and the scattering coefficient of TSM shows a clear linear relationship (Fig. 8), when we omit the measurements of the first day. The scatter diagram of TSM concentration and the particle absorption at 442 nm (Fig. 12) shows a logarithmic relationship, which might be due to changes in the composition of TSM at different concentration levels.

A high correlation was also found for the relationship between total suspended matter dry weight and the Secchi disc depth (Fig. 10). CDOM contributes also to the light penetration, but since its concentration was rather constant during the observation period, the variability in the Secchi disc depth was mainly determined by suspended particles.

BGD
10, 4887–4925, 2013

Of further interest was the relationship between particulate organic carbon and TSM , which is shown in Figs. 13 and 14. These figures show that the 3 samples with very high concentrations of TSM have a relatively lower amount of POC, since they presumably consist of mineralic suspended matter.

Due to the dominating effect of absorption by particulate organic matter and the low chlorophyll concentration, it was difficult to derive the specific phytoplankton pigment absorption coefficient using the filter pad and bleaching method. The relationship between chlorophyll a and the pigment absorption coefficient at 442 nm was: $<\text{chl } a> [\text{mg m}^{-3}] = 7.8$ pigment absorption (apig)_442 nm m^{-1}, which is a lower conversion factor than normally found for open and coastal water phytoplankton.

The relationship between particulate organic carbon and the absorption coefficient of detritus (Fig. 15) has a linear relationship: detritus absorption (a_det) 442 nm $\text{m}^{-1} = 0.83 <\text{POC}> +0.26\ \text{g m}^{-3}$.

Altogether it is possible to establish a first bio-optical model of the Lena water, which can be used for optical remote sensing. This model has linked the concentration of different water constituents with their optical properties. Where a comparison with other areas was possible, in particular with Ob and Yenisei, the values of Lena are similar. Nevertheless, the concentration range of phytoplankton and CDOM was small, which limits the possibility to generalize the results, but since our observation period was during the phase with the maximum run off, the data can be used for estimating the input of substances from the Lena into the coastal water of the Laptev Sea from remote sensing data.

6 Summary and conclusions

The primary goal of this investigation was to determine the bio-optical properties of Lena River water during the phase of maximum run off to get a basis for optical remote sensing and primary production studies. The Investigation site, where we expected maximum concentrations, was the entrance of the Lena Delta before the water enters

BGD
10, 4887–4925, 2013

the coast of the Laptev Sea. The measured variables include absorption and scattering coefficients of water samples before and after filtration to separate the particulate from the dissolved fraction of water constituents. The absorption by particulate matter was further divided by bleaching into absorption coefficients of phytoplankton pigments and detritus. Furthermore, the concentrations of total suspended matter dry weight and of phytoplankton pigments were determined.

Although the short investigation period could provide us only with a snapshot of Lena river optical properties, it was the first time that crucial bio-optical properties of the Lena River were studied during the most dynamic period when the flow and material transportation are maximum. Furthermore, the data were already important for the evaluation of satellite data (Heim et al., 2013).

Most remarkable was the extremely high absorption of light by the dissolved and particulate fraction of humic substances. Secchi disc depths (SD) had a maximum of about 90 cm, which was determined by the dissolved organic matter fraction. This depth was then reduced to 30 cm by variable concentrations of TSM in the range of 8–70 g m^{-3} and with a linear relationship between TSM and SD. However, we expected for this phase of maximum river run off even a higher TSM concentration compared to late summer conditions with low water. In contrast visual turbidity observations in August 2008 in the same area and also satellite data of summer periods indicate a much higher TSM concentration than during this campaign.

The linear relationship between DOC and the absorption coefficient of the filtrate at 442 nm provides the possibility to determine DOC also from optical remote sensing data, from which a_CDOM_442 can be determined (see Heim et al., 2013). More difficult is the determination of particulate carbon (PC) from optical data, since the scattering as well as the absorption coefficient is determined also by particulate matter without carbon.

With respect to the light climate, which is determined by the extremely high absorption in the blue spectral range, the chlorophyll concentration of 1–4 mg m^{-3} was relatively high. Since the water depth of the Lena at the sampling stations was around 6 m

BGD
10, 4887–4925, 2013

with a range of 4–21 m the question arise how phytoplankton can develop under these poor light conditions.

Of interest for remote sensing applications are the spectral slopes of the absorption coefficients of organic matter. The mean value of about 0.015 corresponds to what was found in other estuaries, e.g. the river Elbe (s. introduction). The slight but clear trend over our observation period is presumably due to changes in the composition of organic matter with the river run off. This corresponds to an increase of the absorption by TSM and a decrease of the absorption by dissolved organic matter. Thus, for remote sensing algorithms it might be important to introduce not only one spectral slope but two, which bracket the mean minimum and maximum values.

Since the organic matter is dominating the absorption of Lena water, it will be difficult to identify phytoplankton from reflectance measurements, since its absorption contributes only by less than 10% to the overall absorption.

Although we have sampled only at a few locations and for a short period we expect no significant differences at other locations in the Lena delta during this time, since the environmental conditions elsewhere were very similar, as indicated also by satellite data (Heim et al., 2013).

Our present bio-optical model for the Lena water consists of 4 components:

1. absorption by phytoplankton pigments,
2. absorption by CDOM,
3. absorption by detritus,
4. scattering by TSM.

The mean ranges and conversion factors are:

- Absorption by phytoplankton pigments: range of chlorophyll 0.0–10 $\mathrm{mg\,m^{-3}}$
- Conversion: $<\mathrm{chl}\ a>\,[\mathrm{mg\,m^{-3}}] = 7.8\ a\_\mathrm{pig}\_442\,[\mathrm{m^{-1}}]$

BGD
10, 4887–4925, 2013

- Absorption by CDOM at 442 nm up to 5 m^{-1}
- Spectral slope of CDOM 0.015 ± 0.001

Relationship between DOC [g m^{-3}] and absorption coefficient of CDOM *a* (442 nm) [m^{-1}]:

- *A*_cdom_442 nm [m^{-1}] = 0.56 < DOC> [g m^{-3}]
- Absorption by TSM up to 5 m^{-1}
- Spectral slope of TSM absorption: 0.006 ± 0.001
- Conversion: absorption by TSM: *a*_det_442 [m^{-1}] = 0.07 < TSM > [g m^{-3}]
- Scattering by particles *b*_tsm_442 5–50 m^{-1}
- Conversion: scattering by particles *b*_tsm_442 nm [m^{-1}] = 0.93* < TSM> [g m^{-3}]
- Conversion: particulate carbon [g m^{-3}] and absorption coefficient of bleached particulate matter (detritus) *a*_det_442 nm [m^{-1}] = 0.83 < POC> [g m^{-3}].

Acknowledgements. We are thankful to Günter Stoof and Waldemar Schneider, both Alfred-Wegener-Institute for Polar and Marine Research, who organized the boat trips and all the logistics in the Samoylov station. We are also thanks to Kerstin Heymann for helping the pre-cruise preparation and analyzing the HPLC data and to Bettina Oppermann, Julia Haafke and Saskia Ohse for help with the sampling and analyzing the carbon samples. The research work was supported by the PACES Program of HZG and AWI as well as the ENMAP research program of DLR and the Coastcolour Project of ESA.

References

Babin, M., Stramski, D., Ferrari, G. M., Claustre, H., Bricaud, A., Obolensky, G., and Hoepffner, N.: Variations in the light absorption coefficients of phytoplankton, nonalgal particles, and

BGD
10, 4887–4925, 2013

dissolved organic matter in coastal waters around Europe, J. Geophys. Res., 108, 3211, doi:10.1029/2001JC000882, 2003.
Bélanger, S., Xie, H., Krotkov, N., Larouche, P., Vincent, W. F., and Babin, M.: Photomineralization of terrigenous dissolved organic matter in Arctic coastal waters from 1979 to 2003: Interannual variability and implications of climate change, Global Biogeochem. Cy., 20, GB4005, doi:10.1029/2006GB002708, 2006.
Boss, E., Pegau, W. S., Lee, M., Twardowski, M., Shybanov, E., Korotaev, G., and Baratange, F.: Particulate backscattering ratio at LEO 15 and its use to study particle composition and distribution, J. Geophys. Res., 109, C01014, doi:10.1029/2002JC001514, 2004.
Boss, E., Slade, W. H., Behrenfeld, M., and Dall'Olmo, G.: Acceptance angle effects on the beam attenuation in the ocean, Opt. Express, 17, 153–1550, 2009.
Cauwet, G. and Sidorov, I.: The biogeochemistry of Lena River: organic carbon and nutrients distribution, Mar. Chem., 53, 211–227, 1996.
Dmitrenko, I. A., Sergey, A., Kirillov, L., and Tremblay, B.: The long-term and interannual variability of summer fresh water storage over the eastern Siberian shelf: Implication for climatic change, J. Geophys. Res., 113, C03007, doi:10.1029/2007JC004304, 2008.
Doerffer, R.: Untersuchung über die Verteilung oberflächennaher Substanzen im Elbe-Aestuar mit Hilfe von Fernmessverfahren, Arch. Hydrobiol./Suppl. 43, 119–224, 1979.
Ferrari, G. M., Franco, G. B., and Babin, M.: Geo-chemical and optical characterizations of suspended matter in European coastal waters, Estuar., Coast. Shelf S., 57, 17–24, 2003.
Gueguen, C., Guo, Laodong, and Tanaka, N.: Distributions and characteristics of colored dissolved organic matter in the Western Arctic Ocean, Cont. Shelf Res., 25, 1195–1207, 2005.
Heim, B., Abramova, E., Doerffer, R., Günther, F., Hölemann, J., Kraberg, A., Lantuit, H., Loginova, A., Martynov, F., Overduin, P. P., and Wegner, C.: Ocean Colour remote sensing in the Southern Laptev Sea, Evaluat. Appl., 10, 3849–3889, 2013.
Heiskanen, A. S. and Keck, A.: Distribution and sinking rates of phytoplankton, detritus, and particulate biogenic silica in the Laptev Sea and Lena River, Arctic (Siberia), Mar. Chem., 53, 229–245, 1996.
Helms, J., Stubbins, A., Ritchie, J., D., Minor, E., Kieber, D., and Mopper K.: Absorption spectral slopes and slope ratios as indicators of molecular weight, source, and photo-bleaching of chromophoric dissolved organic matter, Limnol. Oceanogr., 53, 955–969, 2008.

BGD
10, 4887–4925, 2013

Hessen, D., Carroll, J.-L., Kjeldstad, B., Korosov, A., Pettersson, L., Pozdnyakov, D., and Sørensen, K.: Input of organic carbon as determinant of nutrient fluxes, light climate and productivity in the Ob and Yenisey estuaries, Estuar. Coast. Shelf S., 88, 53–62, 2010.

Jerlov, N. G.: A Transparency-Meter for Ocean Water, Tellus, 9, 229–233, 1957.

Kattner, G., Lobbes, J. M., Fitznar, H. P., Engbrod, R., Nötthig, E.-M., and Lara, R. J.: Tracing dissolved organic substances and nutrients from the Lena River through Laptev Sea (Arctic), Mar. Chem., 65, 25–39, 1999.

Korosov, A., Pozdnyakov, D., and Grassl, H.: Spaceborne quantitative assessment of dissolved organic carbon fluxes in the Kara Sea, Adv. Space Res., 50, 1173–188, doi:10.1016/j.asr.2011.10.008, 2011.

Lara, R. J., Rachold, V., Kattner, G., Hubberten, H. W., Guggenberger, G., Skoog A. N., and Thomas, N. D.: Dissolved organic matter and nutrients in the Lena River, Siberian Arctic: Characteristics and distribution, Mar. Chem., 59, 301–309, 1998.

Lobbes, J. M., Fitznar, H. P., and Kattner, G.: Biogeochemical characteristics of dissolved and particulate organic matter in Russian rivers entering the Arctic Ocean, Geochim. Cosmochim. Ac., 64, 2973–2983, 2000.

McClelland, J. W., Déry, S. J., Peterson, B. J., Holmes, R. M., and Wood, E. F.: A pan-arctic evaluation of changes in river discharge during the latter half of the 20th century, Geophys. Res. Lett., 33, L06715, doi:10.1029/2006GL025753, 2006.

Mitchell, B. G., Bricaud, A., Carder, K., Cleveland, J., Ferrari, G., Gould, R., Kahru, Kishino, M., Maske, M. H., Moisan, T., Moore, L., Nelson, N., Phinney, D., Reynolds, R., Sosik, H., Stramski, D., Tassan, S., Trees, C., Weidemann, A., Wieland, J., and Vodacek, A.: "Determination of spectral absorption coefficients of particles, dissolved material and phytoplankton for discrete water samples", in: Ocean Optics Protocols for Satellite Ocean Color Sensor Validation, Revision 2, edited by: Fargion, G. S. and Mueller, J. L., NASA/TM-209966, NASA Goddard Space Flight Center, Greenbelt, Md., 125–153, 2000.

Morison, J., Kwok, R., Peralta, F. C., Alkire, M., Rigor, I., Andersen, R., and Steele, M.: Changing Arctic Ocean freshwater pathways, Nature, 481, 66–70, doi:10.1038/nature10705, 2012.

Payette, S., Delwaide, A., Caccianiga, M., and Beauchemin M.: Accelerated thawing of subarctic peatland permafrost over the last 50 years, Geophys. Res. Lett., 31, L18208, doi:10.1029/2004GL020358, 2004.

Pozdnyakov, D., Korosov, A., Pettersson, L., and Johannessen, O.: MODIS evidences the river run-off impact on the Kara Sea trophy, Int. J. Remote Sens., 26, 3641–3648, 2005.

BGD
10, 4887–4925, 2013

Rachold, V., Alabyan, A., Hubberten, H.-W., Korotaev, V. N., and Zaitsev, A. A.: Sediment transport to the Laptev Sea –Hydrology and geochemistry of the Lena River, Polar Res., 15, 183–196, 1996.

Röttgers, R. and Gehnke S.: Measurement of light absorption by aquatic particles: improvement of the quantitative filter technique by use of an integrating sphere approach, Appl. Optics, 51, 1336–1351, 2012.

Retamal, L., Vincent, W. F., Martineau, C., and Osburn, C. L.: Comparison of the optical properties of dissolved organic matter in two river-influenced coastal regions of the Canadian Arctic, Estuar. Coast. Shelf S., 72, 261–272, 2007.

Sorokin, Y. I. and Sorokin, P. Y.: Plankton and Primary Production in the Lena River Estuary and in the South-eastern Laptev Sea. Estuarine, Coast. Shelf Sci., 43, 399–418, 1996.

Sullivan, J. M., Michael, S. T., Zaneveld, J. R. V., Moore, C. M., Barnard, A. H., Donaghay, P. L., and Rhoades, B.: Hyperspectral temperature and salt dependencies of absorption by water and heavy water in the 400–750 nm spectral range, Appl. Optics, 45, 5294–5309, 2006.

Walsh, J. E.: Arctic as a bellwether, Nature, 352, 19–20, 1991.

Whitmire, A. L., Boss, E., Cowles, T. J., and Pegau, W. S.: Spectral variability of the particulate backscattering ratio, Opt. Express, 15, 7019–7031, 2007.

Wozniak, B. and Dera J.: Light Absorption in Sea Water. Atmospheric and Oceanographic Sciences Library 33, Springer Science and Business Media LLC, 2007.

Zaneveld, J. R. V., Kitchen, J. C., and Moore, C.: The Scattering Error Corection of Reflecting-Tube Absorption Meters, Proc. SPIE, Ocean Optics XII., 2258, 44–55, 1994.

Zapata, M., Rodriguez, F., and Garrido, J. L.: Separation of chlorophylls and carotenoids from marine phytoplankton: a new HPLC method using a reversed phase C8 column and pyridine-containing mobile phases, Mar. Ecol.-Prog. Ser. 195, 29–45, 1994.

BGD
10, 4887–4925, 2013

Table 1. Summary of the phytoplankton composition, size fraction, and total production in the Lena River.

	Picocyanobacteria < 3 µm	Nanophytoplankton 3–10 µm	larger microalgae > 10 µm
Fraction of chl *a* in Lena[a]	0.07	0.16	0.77
Fraction of phae in Lena[a]	0.16	0.21	0.63
Wet weight mg m^{-3}[b]	19	36	407
Prim. Prod. mg C m^{-3} day^{-1}[b]		50–126	
Chl *a* Concentration mg m^{-1}[a]		1.5-4.5	

[a] Heiskanen and Keck (1996)
[b] Sorokin and Sorokin (1996)

BGD
10, 4887–4925, 2013

Table 2. Sampling protocol, Complementary Data and Filtered Volume of the Collected Samples. (Station locations can be found in Fig. 1.)

Location, Time and Station Information					Complementary Data			Filtered Volumes (mL)		
Date	Time (local)	Latitude	Longitude	Station Number	Secchi (cm)	Water Temp.	Air Temp.	TSM	HPLC	PABS
26 Jun 2011	10:00:00	72.37	126.48	2	70	n.a	n.a	500	750	550
26 Jun 2011	15:35:00	72.39	126.64	1	75	n.a	n.a	1000	n.a	1000
27 Jun 2011	10:30:00	72.37	126.48	2	70	13		1000	1000	1000
27 Jun 2011	15:30:00	72.39	126.64	1	60	13.2	7.5	1000	1000	1000
28 Jun 2011	10:50:00	72.33	126.29	6	80	12.5	8.2	1000	1000	500
28 Jun 2011	11:20:00	72.35	126.33	5	85	12.3	9.5	1000	1000	500
28 Jun 2011	11:53:00	72.37	126.38	4	80	12.2	8.4	1000	1000	500
28 Jun 2011	12:10:00	72.38	126.43	3	75	12.2	8.6	1000	1000	500
29 Jun 2011	10:30:00	72.37	126.48	2	75	13.5	8.8	1500	n.a	n.a
29 Jun 2011	15:30:00	72.39	126.66	1	70	13.6	8.9	1500	1500	500
30 Jun 2011	10:30:00	72.37	126.48	2	n.a	n.a	n.a	1500	1500	500
30 Jun 2011	15:30:00	72.39	126.64	1	n.a	n.a	n.a	1500	1000	500
1 Jul 2011	10:30:00	72.37	126.48	2	70	13.4	7.3	1500	1000	500
1 Jul 2011	16:00:00	72.39	126.64	1	70	13	8.5	1500	1500	500
2 Jul 2011	10:30:00	72.37	126.48	2	70	13.3	8.4	1500	1000	500
2 Jul 2011	15:50:00	72.39	126.66	1	50	13.3	12	1000	1000	250
3 Jul 2011	19:30:00	72.37	126.46	2	35	13.7	17.8	700	700	200
3 Jul 2011	20:00:00	72.39	126.66	1	30	13.8	16	700	700	200
4 Jul 2011	09:00:00	72.37	126.47	2	40	14	18	1000	1000	250
4 Jul 2011	15:30:00	72.39	126.66	1	30	14.2	17.9	700	700	200

n.a: not available.

BGD
10, 4887–4925, 2013

Table 3. Columns CDOM and DETRITUS are the spectral slopes of CDOM and detritus. The corresponding concentrations are listed in columns TSM (total suspended matter dry weight in mg L^{-1}) and Chl *a* (chlorophyll including all degradation products in µg L^{-1}

Date	Time (local)	CDOM	DETRITUS	TSM	Chl *a*
26 Jun 2011	10:00:00	No Data	0.00622	15.06	0.920
26 Jun 2011	15:35:00	0.014323	0.006039	21.66	No Data
27 Jun 2011	10:30:00	0.014676	0.00527	19.51	2.184
27 Jun 2011	15:30:00	0.014781	0.004893	30.42	2.100
28 Jun 2011	10:00:00	No Data	No Data	15.43	No Data
28 Jun 2011	10:50:00	0.014859	0.008914	7.92	0.939
28 Jun 2011	11:20:00	0.014801	0.008649	9.36	1.610
28 Jun 2011	11:53:00	0.014711	0.00866	9.08	0.315
28 Jun 2011	12:10:00	0.014816	0.008331	8.45	2.306
29 Jun 2011	10:30:00	No Data	No Data	24.27	No Data
29 Jun 2011	15:30:00	0.014849	0.005714	27.25	2.043
30 Jun 2011	10:30:00	0.015026	0.004277	52.94	2.904
30 Jun 2011	15:30:00	0.014944	0.004771	37.34	2.995
1 Jul 2011	10:30:00	0.014958	0.005967	25.87	2.902
1 Jul 2011	16:00:00	0.015219	0.005387	28.63	1.930
2 Jul 2011	10:30:00	0.015159	0.005364	25.95	2.215
2 Jul 2011	15:50:00	0.015241	0.004244	54.77	1.888
3 Jul 2011	19:30:00	0.015369	0.004785	55.58	1.336
3 Jul 2011	20:00:00	0.01559	0.003884	58.81	1.380
4 Jul 2011	09:00:00	0.014992	0.003885	48.77	1.613
4 Jul 2011	15:30:00	0.015324	0.004056	**67.59**	1.192
Mean		**0.01498**	**0.005753**	**31.89**	**1.820627**
Std		**0.0003**	**0.001688**	**19.94**	**0.733779**

BGD
10, 4887–4925, 2013

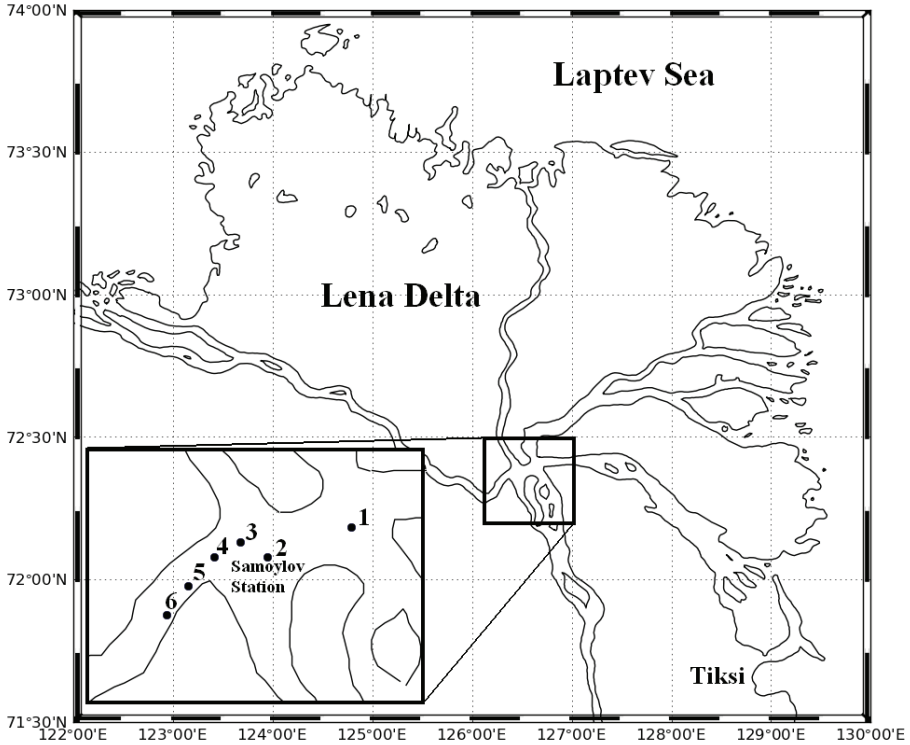

Fig. 1. Study area and location of sampling stations.

BGD
10, 4887–4925, 2013

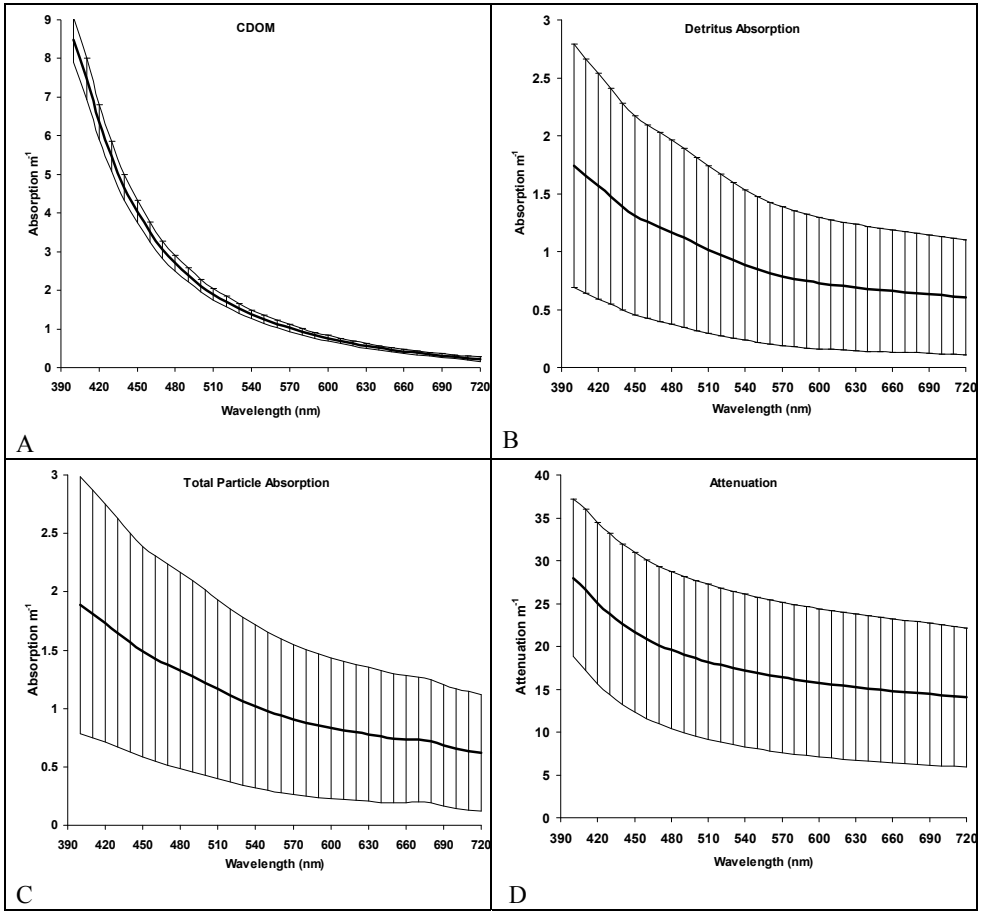

Fig. 2. Mean, CDOM m^{-1} **(A)**, Detritus m^{-1} **(B)**, Total Particle Absorption m^{-1} **(C)** and Attenuation **(D)** m^{-1} with standard deviation.

BGD
10, 4887–4925, 2013

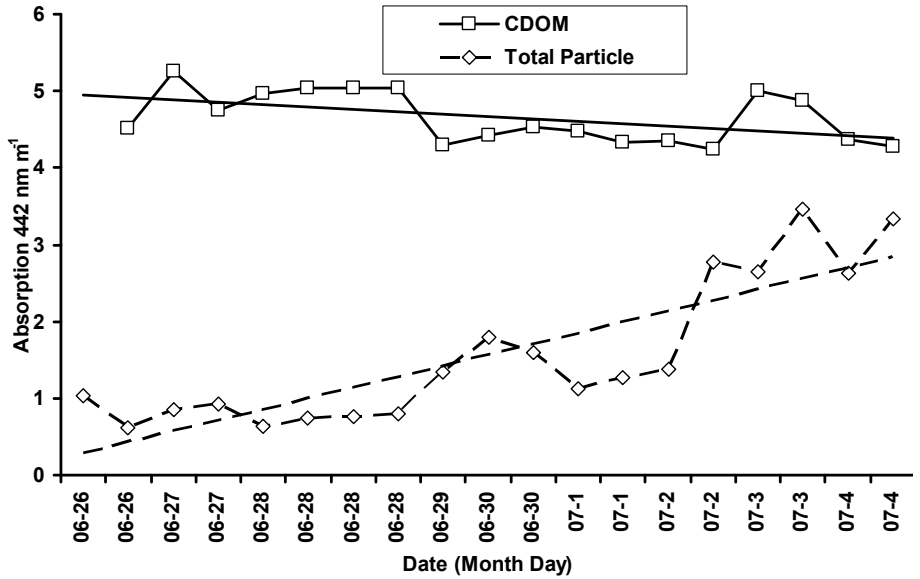

Fig. 3. CDOM and Total Particle Absorption variability at 442 nm during the sampling period.

BGD
10, 4887–4925, 2013

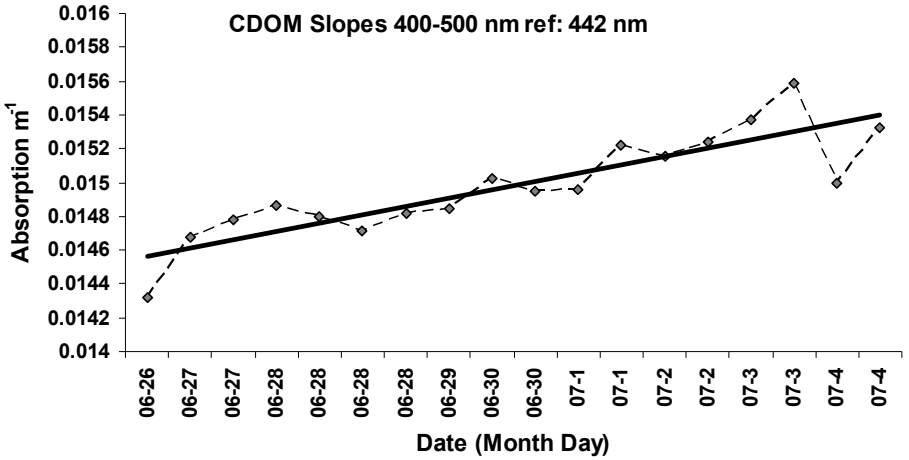

Fig. 4. CDOM semi-logarithmic slopes calculated between 400 to 500 nm with 442 nm reference wavelength.

BGD
10, 4887–4925, 2013

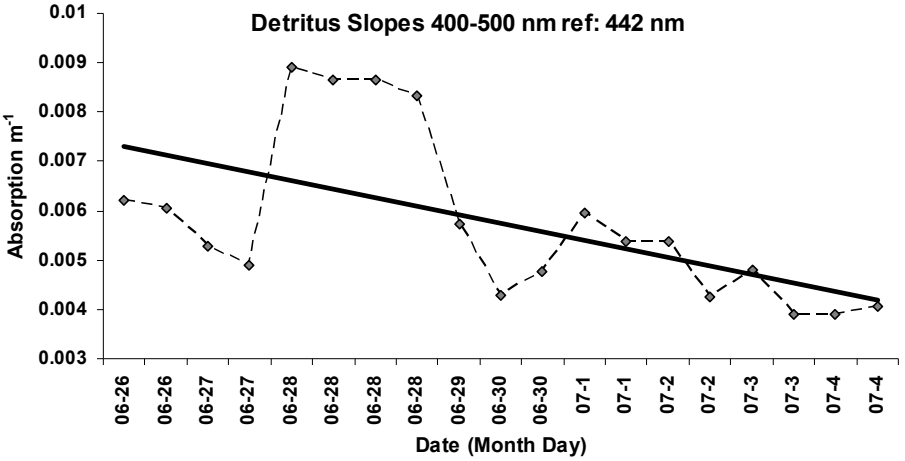

Fig. 5. Detritus, semi-logarithmic slopes calculated between 400 to 500 nm with 442 nm reference wavelength.

BGD
10, 4887–4925, 2013

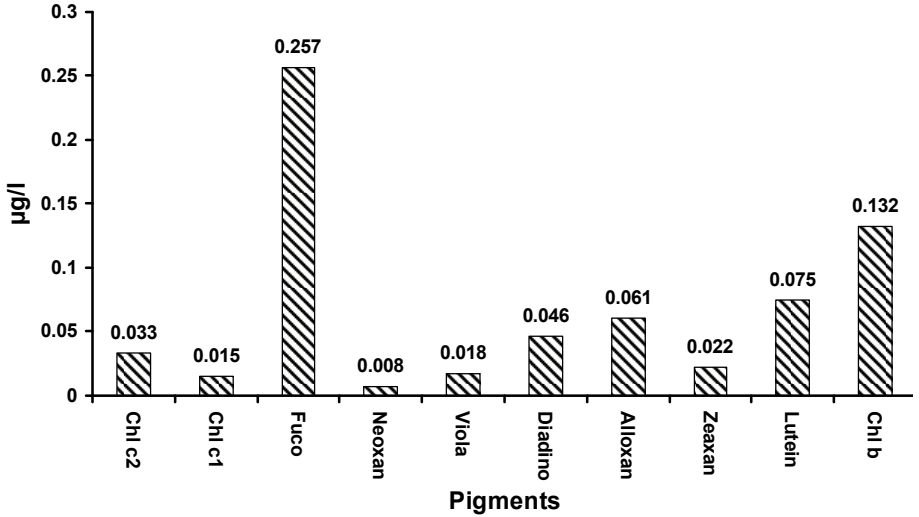

Fig. 6. Mean pigment concentrations.

BGD
10, 4887–4925, 2013

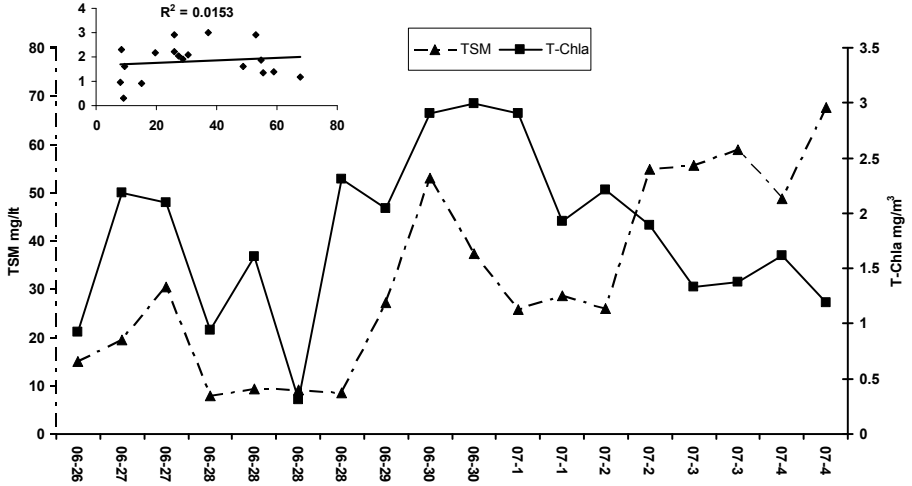

Fig. 7. Temporal fluctuations of the total chlorophyll *a* and total suspended matter and their relation (top left).

BGD
10, 4887–4925, 2013

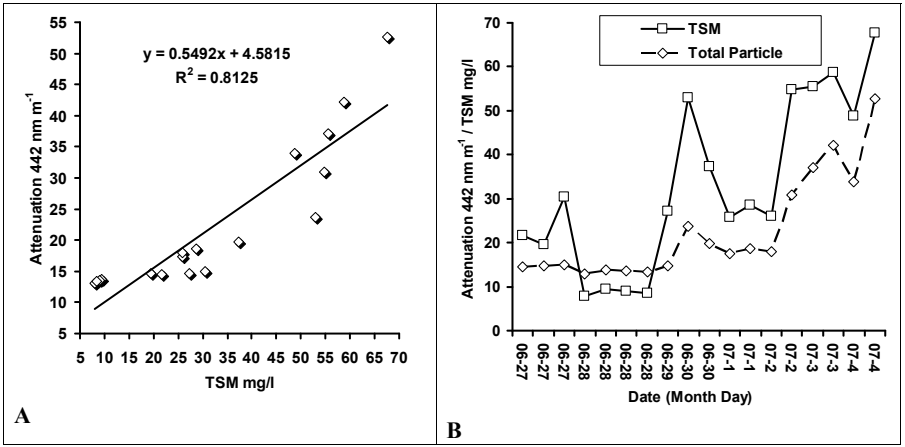

Fig. 8. Co-variation of TSM mg L^{-1} and Attenuation m^{-1} at 442 nm **(A)**, and temporal variation of the TSM values mg L^{-1} and Attenuation m^{-1} at 442 nm **(B)**.

BGD
10, 4887–4925, 2013




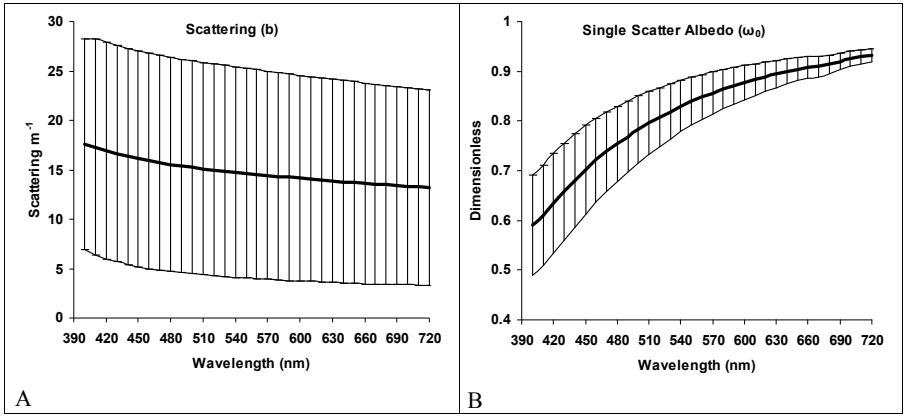

Fig. 9. (A) Scattering b , **(B)** Single Scatter Albedo (ω_0), means and standard deviations.

BGD
10, 4887–4925, 2013

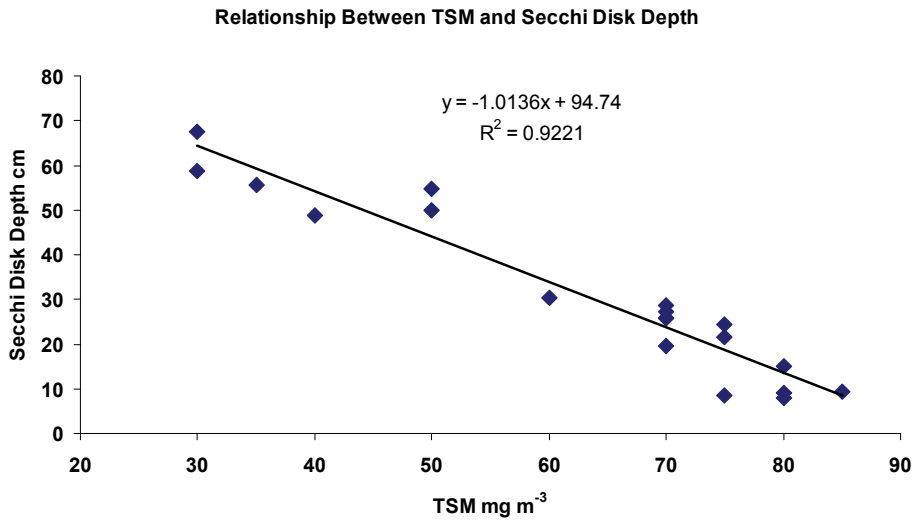

Fig. 10. Relationship between Total suspended Matter (TSM) dry weight and the Secchi disc depth for all Lena stations.

BGD
10, 4887–4925, 2013

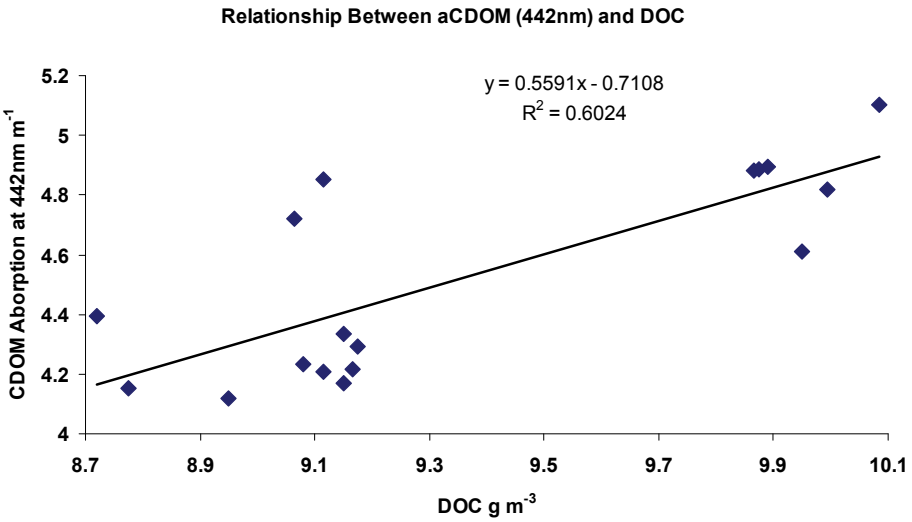

Fig. 11. Relationship between DOC and the absorption coefficient of the filtrate at 442 nm against pure water as blank.

BGD
10, 4887–4925, 2013

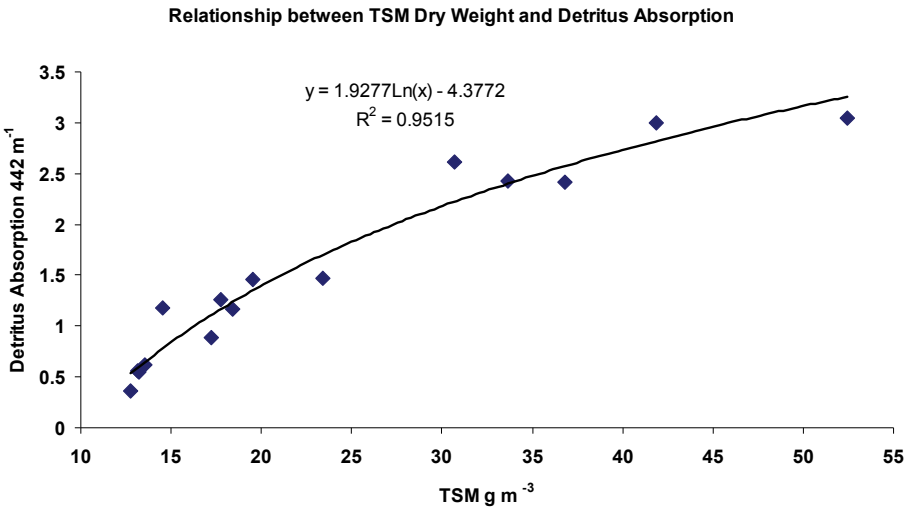

Fig. 12. Relationship between totals suspended matter dry weight (TSM) and the absorption coefficient of the particulate matter at 442 nm.

BGD
10, 4887–4925, 2013

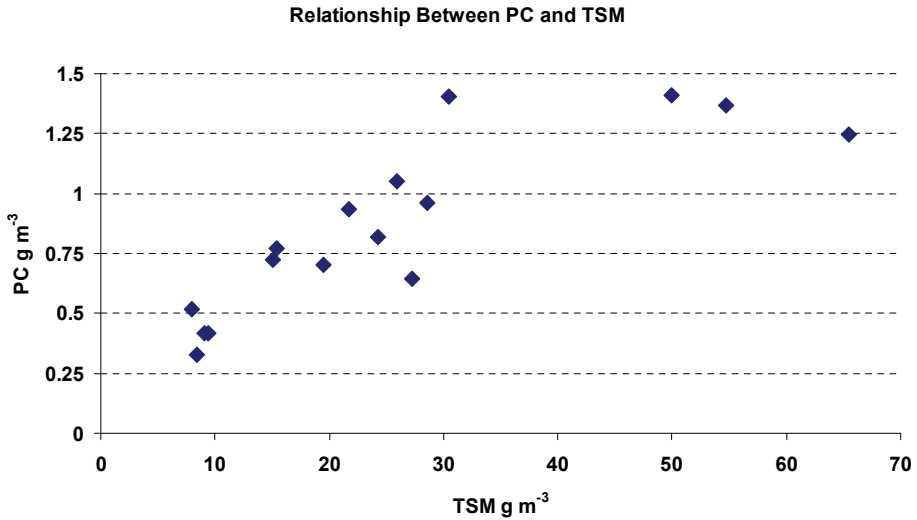

Fig. 13. Relationship between weight particulate carbon and total suspended matter.

BGD
10, 4887–4925, 2013

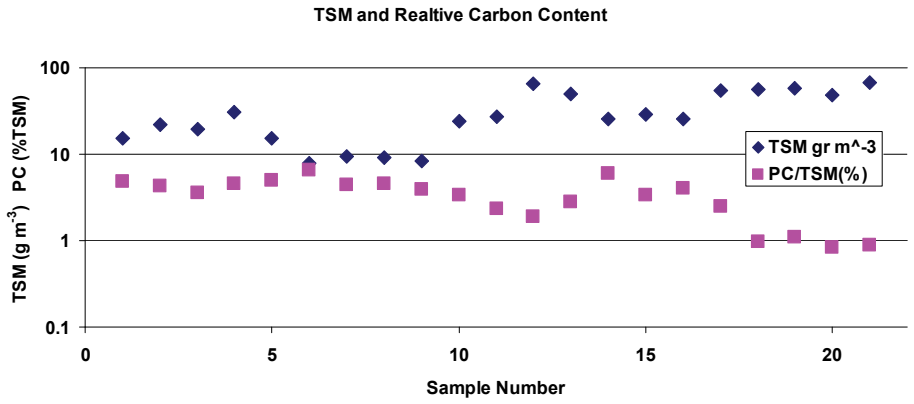

Fig. 14. Total suspended matter dry weight (TSM) in g m^{-3} and the particulate carbon content in % in sequence of sample number.

BGD
10, 4887–4925, 2013

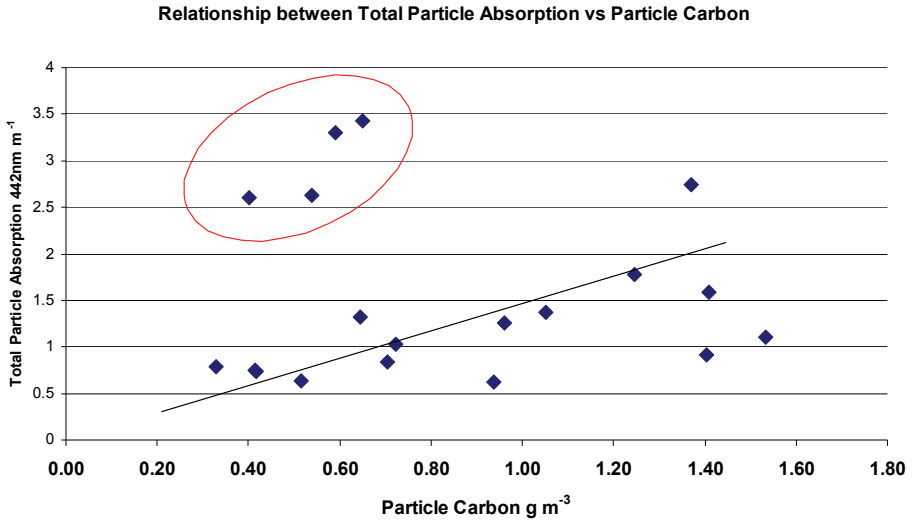

Fig. 15. Relationship between particulate carbon (PC) and the absorption coefficient of particulate matter at 442 nm, data points within red circle are only from samples of 3 and 4 July 2011, when omitting these points the regression is $y = 0.83\,x + 0.26$.

BGD
10, 4887–4925, 2013